

Enhanced photocatalytic activity of ZnO nanoparticles grown on porous silica microparticles

M. S. Azmina¹  · R. Md Nor¹ · H. A. Rafeaie² · N. S. A. Razak¹ · S. F. A. Sani¹ · Z. Osman¹

Received: 5 September 2017 / Accepted: 1 November 2017 / Published online: 13 November 2017
© The Author(s) 2017. This article is an open access publication

Abstract ZnO nanoparticles (NPs) have been synthesized on porous silica microparticles, namely sand microparticles using the sol–gel technique. The ZnO NPs grown on the multifaceted surface of porous silica microparticles were applied as photocatalyst for the degradation of methylene blue (MB) in aqueous solution. The enhanced rate constant observed was due to two reasons. Firstly, the multifaceted surface of the sand substrate provided fixed space for growth space which prevented agglomeration of the ZnO NPs photocatalyst, thus maintaining a large surface area. Secondly, the presence of nanopores on the sand surface provided adsorption sites for MB molecules to be in the vicinity of the photocatalyst. The photocatalytic activity was significantly enhanced where photodegradation efficiency of supported ZnO NPs reached 71.7% compared to 48.2% for unsupported ZnO NPs under UV light irradiation within 150 min. The values of k increased from $4.3 \times 10^{-3} \text{ min}^{-1}$ to $8.6 \times 10^{-3} \text{ min}^{-1}$ for unsupported and supported ZnO NPs, respectively.

Keywords Photocatalyst · Zinc oxide · Nanoparticles · Photodegradation · Porous silica

Electronic supplementary material The online version of this article (<https://doi.org/10.1007/s13204-017-0626-3>) contains supplementary material, which is available to authorized users.

✉ M. S. Azmina
nurazminasafian@yahoo.com

¹ Department of Physics, Faculty of Sciences, University of Malaya, 50603 Kuala Lumpur, Malaysia

² Unit of Physics, School of Science, Universiti Teknologi MARA (UiTM) Pahang Branch, Campus Jengka, 26400 Bandar Tun Abdul Razak Jengka, Pahang, Malaysia

Introduction

Nanomaterials possess unique and beneficial chemical, physical and mechanical properties which can be used for a wide variety of applications. However, the greatest technical challenge in the application of nanoparticles is agglomeration. The high surface area to volume ratio of nanoparticles resulted in very high surface energy (Nanda et al. 2003). To minimize its surface energy, the nanoparticles tend to agglomerate (Tang et al. 2006). Uncontrolled agglomeration of nanoparticles occurs due to strong van der Waals attraction forces between particles (Cao 2004). In nanomaterials, the percentage of surface atoms are high, resulting in enhanced particle reactivity (Gilbert et al. 2004; Roduner, 2006). This causes nanoparticles to adhere among themselves and to other materials, including container walls. The agglomeration of nanomaterials will inevitably diminish the expected benefit of the size effect.

Many techniques have been employed to overcome the problem of nanoparticle agglomeration. These include the use of surfactants (Ortiz Landeros et al. 2012; Zhang et al. 2009), emulsification (Binks et al. 2010; Noshirvani et al. 2017) external forces (Bandeekar et al. 2014; Guo et al. 2016; Sauter et al. 2008) and the use of substrates (Miao et al. 2007; Zhang, Xue and Wang 2002). In principle, nanoparticles synthesized on substrates will be fixed in space and agglomeration can be prevented (Sun and Siringhaus 2006). Examples of conventional substrates used are glass (Mamat et al. 2010; Zhang et al. 2002) and silicon (Kuo et al. 2007; Lin, Fu and Jia 2001). The control over either agglomeration of nanoparticles or adhesion of nanoparticles remains the major problem, especially for photocatalysis application. A porous substrate is an alternative and promising way to improve the adhesion of

nanoparticles. The pores limit the size of nanoparticles and provide excellent adhesion to the nanoparticles.

ZnO as a photocatalyst afforded several advantages such as being photocatalytically more active than others (Jang et al. 2006) and having excellent chemical and photochemical stability, non-toxicity (Amna et al. 2015; Pung ET AL. 2012), low cost and large exciton binding energy (60 meV) for nanoparticles (Mollwo 1982). In nanoparticle form, ZnO is expected to provide significantly enhanced reactivity due to increased specific area and changes of the surface properties of the sample (Dodd et al. 2006).

In this paper, we present the results of a study on the use of porous silica microparticles, namely sand microparticles as substrates for the growth of ZnO nanoparticles (NPs). Sand microparticles were chosen due to the presence of nanosized pores which provide physical space for the dye solution to be temporarily adsorbed during the photodegradation process. Good adhesion of the ZnO NPs during the growth process is facilitated, due to the presence of nanosized pores, pits and lines at the surface of the sand. The photodegradation efficiency of supported ZnO NPs to unsupported ZnO NPs of similar size and under similar conditions was compared to evaluate the effect of agglomeration in unsupported ZnO photocatalyst on the photodegradation efficiency.

Experimental method

Preparation of porous silica microparticles

River sand particles with sizes between 200 and 500 μm were soaked in acetone under stirring for 24 h to remove organic materials. After rinsing in deionized (DI) water, the sand particles were soaked in sulfuric acid for 24 h to remove metallic and inorganic materials. Lastly, the sand particles were sonically cleaned in methanol and DI water, followed by drying on a hot plate.

Synthesis of supported ZnO nanoparticles on porous silica microparticles

Before deposition, the cleaned sand microparticles were seeded with a very thin ZnO layer. This is achieved by three cycles of soaking in a 0.005 M zinc acetate solution and annealing at 300 °C. Deposition of ZnO was by the chemical method using 0.05 M of zinc nitrate hexahydrate and 0.05 M hexamethylenetetramine (HMTA), both in DI water. The solution was set at pH 8 by adding 1.0 M sodium hydroxide (NaOH) solution. 5 g of sand microparticles was added to the growth solution, which was stirred continuously at 100 °C for 6 h. Then, the solution was continuously stirred for a further 12 h at room

temperature for the aging process. Sand microparticles deposited with ZnO NPs were extracted from the solution by sieving to remove loose ZnO NPs before being annealed at 300 °C for 2 h. X-ray diffraction (XRD), field emission scanning electron microscopy (FESEM) and transmission electron microscopy (TEM) were used to characterize the samples. The amount of ZnO NPs deposited was estimated by comparing the weight of similar volumes of the sand deposited with ZnO NPs and clean sand samples.

Synthesis of unsupported ZnO nanoparticles

Unsupported ZnO NPs (loose ZnO NPs) were synthesized using equal volumes of 0.01 M of zinc nitrate hexahydrate as the zinc source and 0.01 M of HMTA as a stabilizer, both dissolved in DI water. The mixed solution was stirred at 100 °C for 6 h, then cooled to room temperature and extracted from the solution. The ZnO NPs powder obtained was calcined at 300 °C for 2 h on a hot plate and then characterized using XRD and FESEM.

Photodegradation of methylene blue under ultraviolet (UV) light

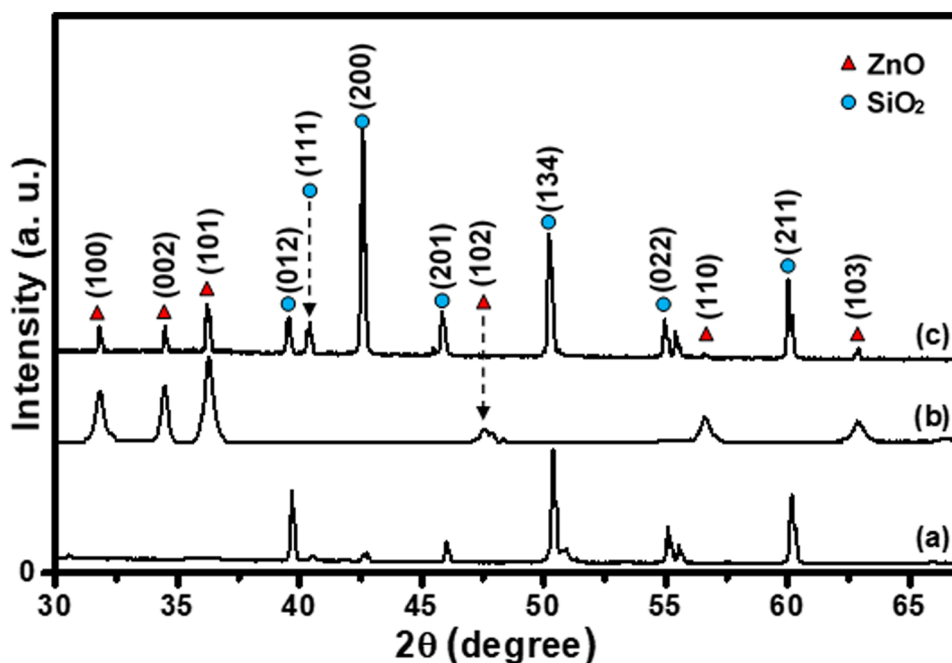
The photocatalytic degradation of methylene blue (MB) was performed under UV light at 254 nm. 30 mg unsupported ZnO NPs and the weight equivalent of supported ZnO NPs were used as the photocatalysts. The equivalent weight was determined based on a calibration process described in section S1 in the electronic supplementary document. The initial concentration of the MB solution was 5 mg/L. Before the photodegradation process, the MB solutions containing the photocatalysts were stirred in the dark until equilibrium absorption of MB on the photocatalysts occurred as shown in Figure S2 in the electronic supplementary document. Then, the photodegradation process commenced under UV light irradiation for a duration up to 150 min. At 15 min interval, about 4 ml of the solution was extracted and centrifuged to remove ZnO NPs. UV–Vis absorption spectrometry was performed on the extracted MB solution where its concentration was estimated based on the characteristic MB UV–Vis absorption peak at 664 nm. For comparison, photodegradation experiments using supported ZnO NPs without irradiation and sand under UV as well as without UV were also performed.

Results and discussions

Structure and morphology

The XRD spectra of sand microparticles, unsupported ZnO NPs and supported ZnO NPs are shown in Fig. 1. The XRD

Fig. 1 XRD patterns of the **a** sand microparticles, and **b** unsupported and **c** supported ZnO NPs synthesized for 6 h using the sol–gel method



peaks from the sand microparticle sample shown as trace (a) gave peaks at 39.67° , 40.38° , 42.59° , 45.9° , 50.38° , 55.11° and 60.11° , which were attributed to the (012), (111), (200), (201), (134), (022) and (211) reflection planes of quartz, based on the JCPDS file no. 46-1045. No peaks due to other crystalline materials were observed. Trace (b) shows the XRD peaks due to the unsupported ZnO NPs. Peaks at 31.81° , 34.45° , 36.33° , 47.62° , 56.60° and 62.88° can be attributed to the (100), (002), (101), (102), (110) and (103) reflection plane of ZnO, based on the JCPD card 79-2205. In trace (c), all peaks due to ZnO and quartz mentioned above were detected, indicating the growth of ZnO on the microsized sand particles.

Detailed analysis of the XRD results are given in section S3 in the electronic supplementary document. In Table S1, which shows an evaluation of the preferential orientation of the samples, a slight orientation preference to the (100), (002) and (101) planes is given for the supported ZnO NPs samples when compared with the standard ZnO powder sample. Also, some variation was observed. Crystallite size based on estimations using the Scherrer equation showed slightly bigger crystallites of ZnO NPs grown on sand compared to unsupported ZnO NPs (see Table S2). These factors are unlikely to affect the photocatalytic activity, which depends on the band gap and the defect levels of the photocatalyst.

Figure 2 shows the typical FESEM images of sand microparticles, and supported and unsupported ZnO NPs samples. Figure 2a shows the morphology of sand with particle size of between 200 and 500 μm . It clearly showed that the sand was structured with multifaceted surfaces and

surrounded with nanopores. Figure 2b is a low-resolution image showing the growth of the ZnO NPs on the surface of microsized sand particles. The image of unsupported ZnO nanoparticles is shown in Fig. 2c. A close-up view of the supported ZnO NPs is shown in Fig. 2d. Based on the images, the particles sizes were estimated to be between 37.5 and 76.2 nm for unsupported ZnO NPs and 33.8–89.8 nm for supported ZnO NPs.

Figure 3 shows the TEM images of ZnO NPs on microscopic sand. The high-resolution image, as in Fig. 3c, shows that the ZnO NPs with interplanar spacing of 0.26 nm adhered seamlessly to the sand particles. This value corresponds to the d-spacing of the ZnO (002) plane and indicates that ZnO NPs grew in the direction of [0001]. Continuous growth of ZnO NPs occurred on the sand particles, and it seemed that the ZnO NPs grew out of nanosized pits and craters on the surface of the sand particles. This demonstrated that ZnO NPs efficiently adhered to the sand particles.

Photocatalytic activity

UV light may cause degradation of methylene blue molecules even without catalysts. To test the extent of degradation afforded by UV light, we exposed MB solution to UV light. The results are shown in Figure S3 in section S4 in the electronic supplementary document, which indicated that degradation due to UV light alone was negligible.

Figure 4 shows the time evolution of the UV–Vis spectra of MB solution at about 664 nm in the photodegradation experiments using sand, and supported and

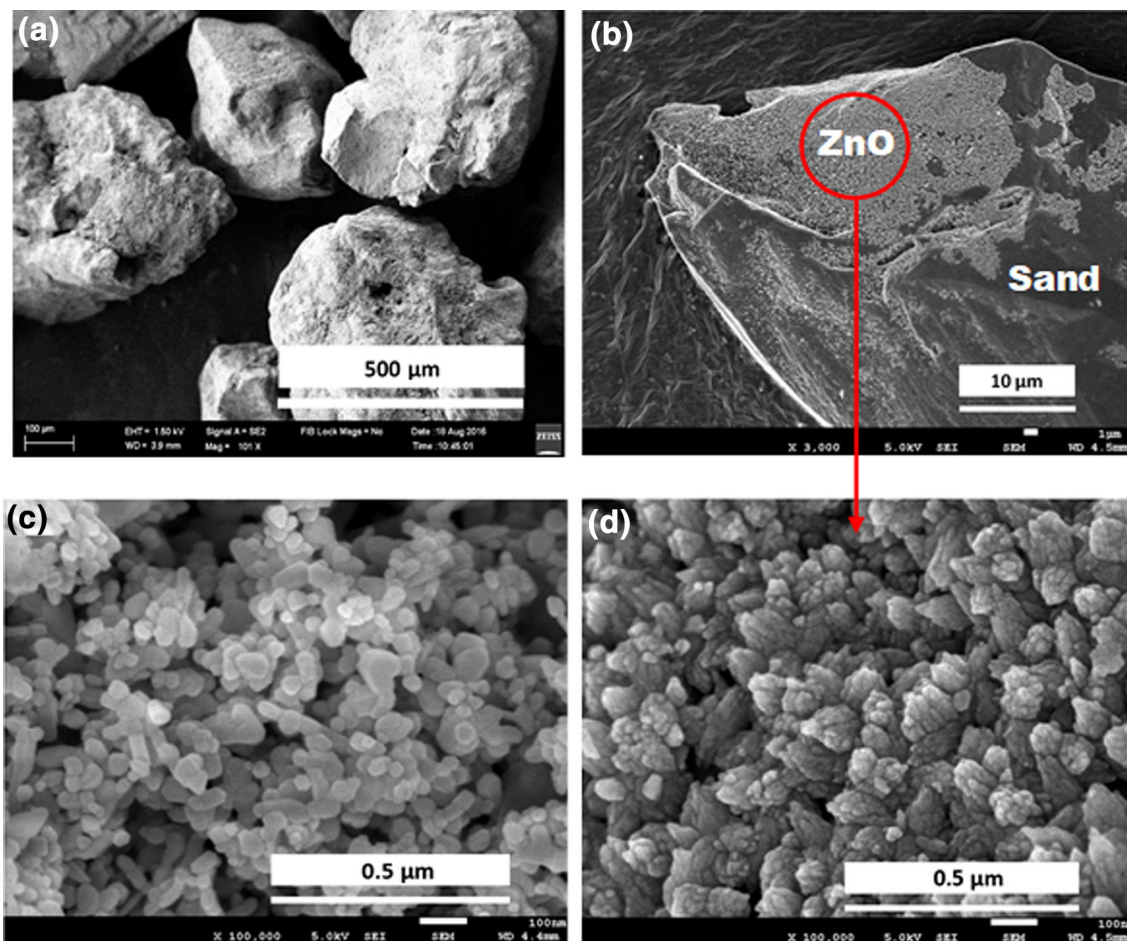


Fig. 2 FESEM images of **a** sand microparticles and **b** supported ZnO NPs. The agglomeration of nanoparticles for **c** unsupported and **d** supported ZnO NPs

unsupported ZnO NPs, all under 254 nm under UV light irradiation, as well as results using supported ZnO NPs but kept in the dark as control. The peak height of the MB UV–Vis characteristic peak at 664 nm was taken as the relative concentration of MB in the solution.

Figure 5 shows the time-varying plot of the degradation percentage of MB due to the photodegradation process. The photodegradation efficiency (%) defined as the maximum photodegradation at 150 min was calculated as follows:

$$\begin{aligned} \text{Photodegradation efficiency (\%)} &= \left(\frac{C_0 - C_{150}}{C_0} \times 100 \right) \\ &= \left(\frac{A_0 - A_{150}}{A_0} \right) \times 100, \end{aligned} \quad (1)$$

where C_0 and C_{150} are the concentrations of MB at $t = 0$ and $t = 150$ min, respectively, while A_0 and A_{150} represent the intensity of MB characteristic absorption wavelength 664 nm at $t = 0$ and $t = 150$ min, respectively (Xu et al. 2008).

Here, the change between the values of A_0 and A_{150} which were the initial (at $t = 0$) and final (at $t = 150$ mins) peak heights of the characteristic MB UV–Vis absorption using supported ZnO NPs, respectively, but kept in the dark was about 14.7% as shown in Fig. 5. This was due to the adsorption of MB molecules on the photocatalyst surface. Pure sand particles under UV light irradiation and without irradiation yielded a maximum removal of 15.6 and 15.3%, respectively. The slight increase was due to the greater efficiency of MB adsorption on sand than on ZnO, though there was a possibility of the presence of a trace amount of photocatalysts, such as iron oxide, which were not detected in the XRD analysis. Here, the use of sand particles as support for ZnO NPs photocatalyst seemed to enhance the adsorption of MB on or in the vicinity of the photocatalyst. Maximum photodegradation of 48.2% was obtained when unsupported ZnO NPs was used. With supported ZnO NPs, a value of 71.7% was obtained, providing an increase of almost 49%. There can be three possible reasons for the enhancement. First, the nanoparticles were on the sand surface and were prevented from

Fig. 3 TEM images of supported ZnO NPs at **a** 100 nm, **b** 50 nm and **c** 5 nm scale bars

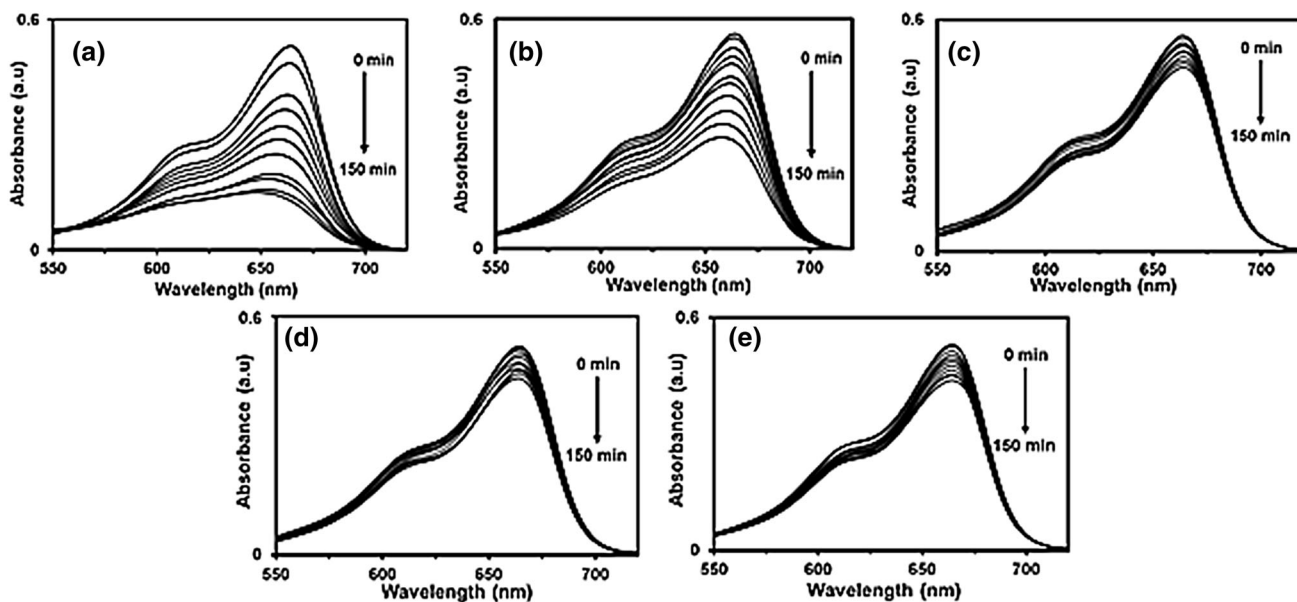
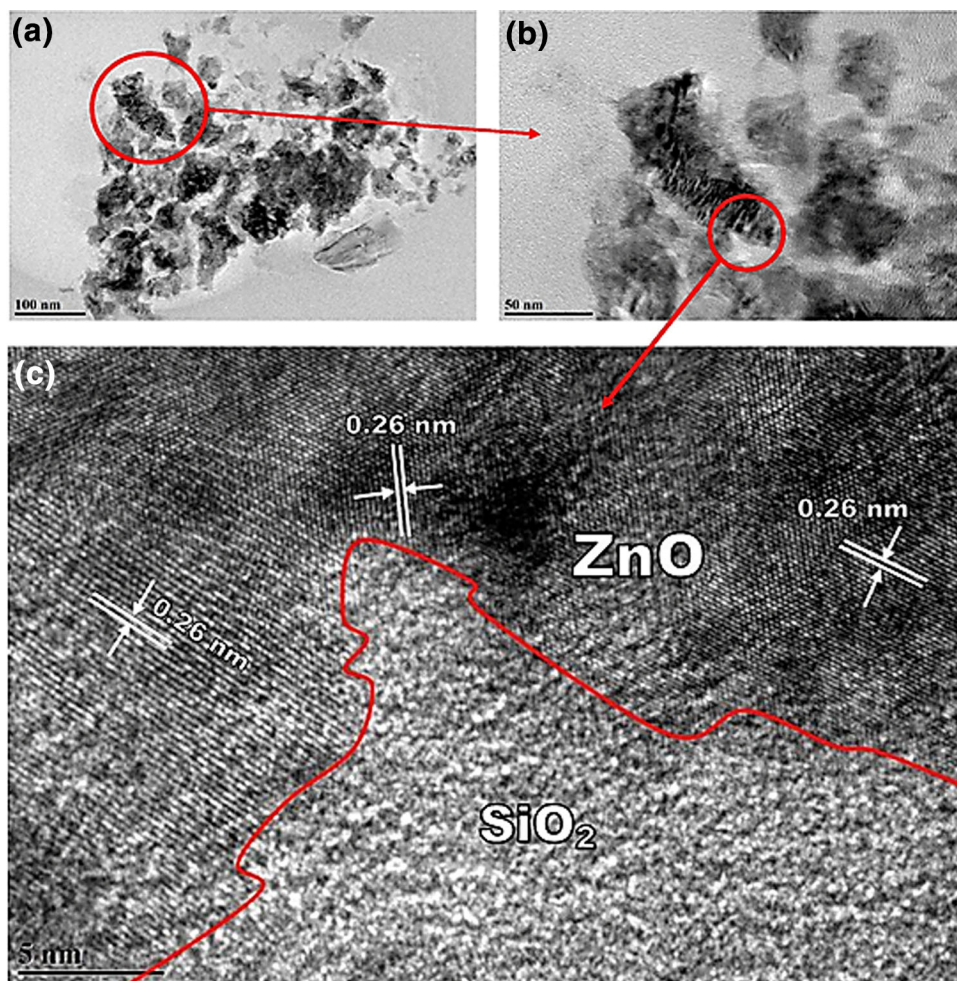


Fig. 4 The time evolution of the UV-Vis spectra of MB taken at 15 min intervals for **a** supported ZnO NPs with UV, **b** unsupported ZnO NPs with UV, **c** supported ZnO NPs in the dark, **d** clean sand in

the dark and **e** clean sand with UV light irradiation. Experimental conditions: amount of catalyst 30 mg and initial MB concentration 5 mg/L

Fig. 5 Photodegradation efficiency curves of MB degradation using sand microparticles, supported ZnO NPs and unsupported ZnO NPs for 150 min irradiation time

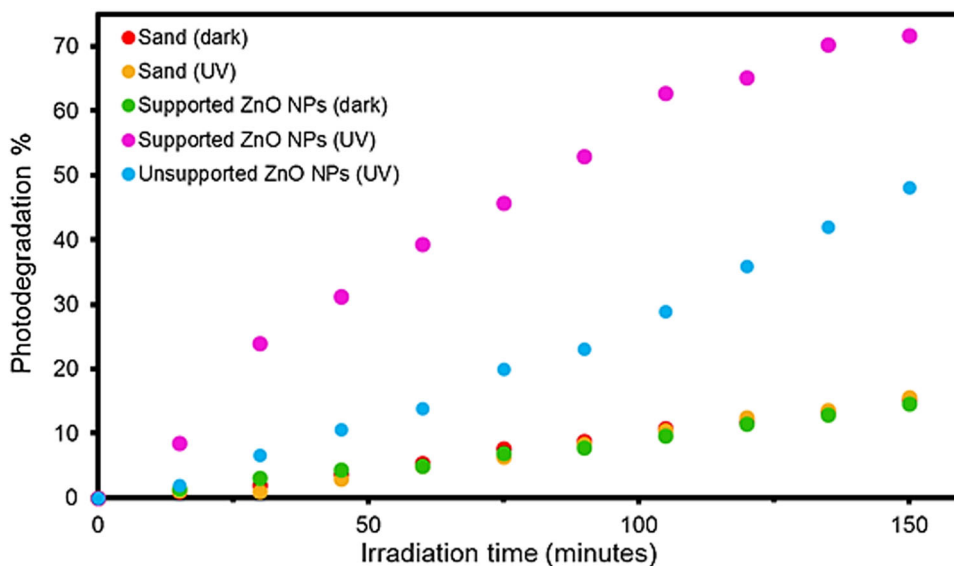
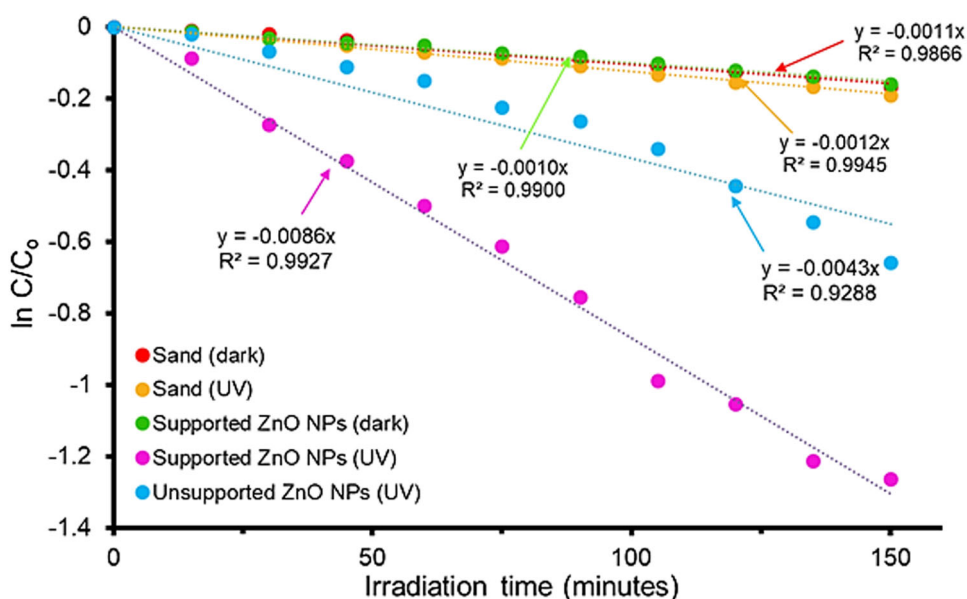


Fig. 6 Plots of $\ln(C/C_0)$ versus irradiation time for the photodegradation processes of MB using sand, supported ZnO NPs and unsupported ZnO NPs as photocatalysts. Experimental conditions: amount of catalyst 30 mg and initial MB concentration 5 mg/L



agglomerating. Second, the microsized sand particles suspended in the solution under stirring provided less scattering effect of the UV light used. Third, as mentioned earlier, MB are more efficiently adsorbed in the vicinity of the ZnO NPs photocatalyst deposited on sand than on unsupported ZnO NPs.

The degradation of dye can be described by the pseudo-first-order equation with the simplified Langmuir–Hinshelwood model:

$$C = C_0 \exp(-kt). \quad (2)$$

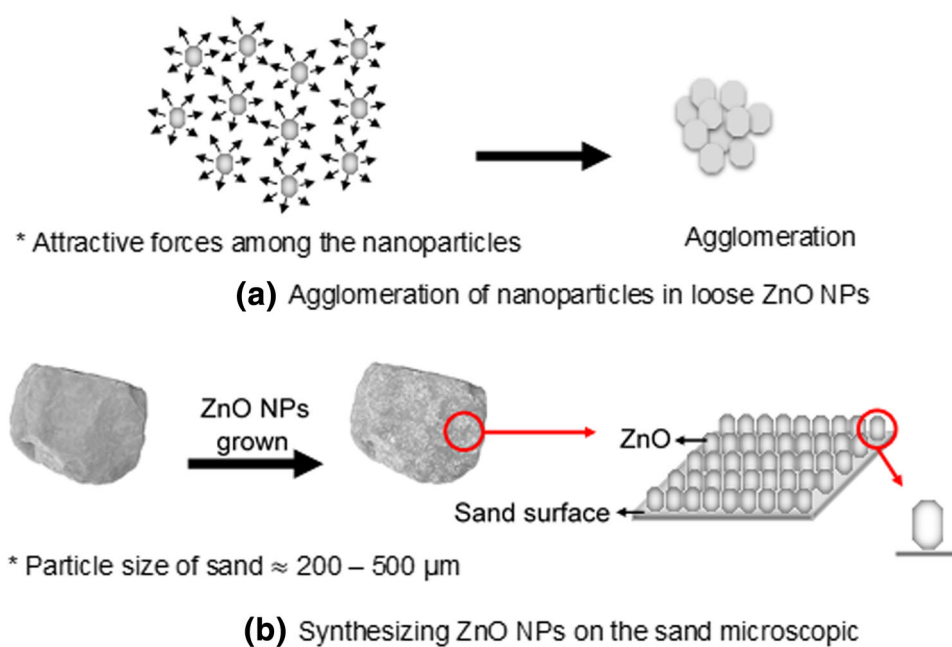
In linear form:

$$\ln\left(\frac{C}{C_0}\right) = -kt, \quad (3)$$

where C_0 is the MB initial concentration, C is the concentration of the MB solution after the degradation time, and t and k are the photodegradation rate constant. The linear plot of $\ln(C/C_0)$ versus t for degradation of MB solution using unsupported ZnO NPs photocatalyst kept in the dark and sand, unsupported ZnO NPs and ZnO NPs on sand microparticles are shown in Fig. 6. From the linear fittings, the values of the photodegradation rate constant were obtained.

The results showed that the supported ZnO NPs under UV light irradiation gave the highest photocatalytic performance, where the value of k was $8.6 \times 10^{-3} \text{ min}^{-1}$ compared to unsupported ZnO NPs ($4.3 \times 10^{-3} \text{ min}^{-1}$). Here, the k value using supported ZnO was double that of

Fig. 7 Illustration of the effect of agglomeration and how synthesis on substrates fixed the nanoparticles in space and prevented agglomeration



the unsupported sample, thus demonstrating that using microsized support the nanosized effect of the ZnO NPs was better utilized than in the unsupported form, where agglomeration was expected to be more prevalent. Another advantage is that the supported ZnO NPs can be more easily recovered for reuse. Also, we demonstrated the efficiency of using microsized sand particles as support for ZnO NPs which provided good adhesion of ZnO NPs and good adsorption of MB molecules during the photocatalysis process.

The used of sand microparticles as template for ZnO NPs growth placed the MB molecules in the vicinity of the photocatalyst. Figure 7 shows an illustration of how agglomeration of nanoparticles in loose powder occurred. The agglomeration of nanoparticles mainly occurred due to high surface energy, high surface tension and strong van der Waals forces. During the synthesis process, primary particles with sizes less than 100 nm were produced. In this stage, greater interaction between nanoparticles and higher attractive forces occurred due to high surface area. The high attractive forces of reactive nanoparticles cause a strong adhesion between nanoparticles and consequently lead to the agglomeration of nanoparticles. A strong adhesion between nanoparticles can be reduced by providing a substrate to immobilize the nanoparticles.

Achak et al. (2009) reported applying sand as a filter to remove up to 60% of organic pollutants and nutrients from olive mill wastewater. According to Tao and Mancl (2008), the ideal particle sizes of sand for intermittent bioreactors are medium to coarse sand with an effective size in the range of 0.3–1.5 mm. The pores will not only

provide a surface with good adhesion for ZnO NPs growth, but also adsorb MB molecules in the vicinity of the ZnO NPs photocatalyst, which will further enhance the photodegradation process. The oxidation and reduction process is accelerated by the reaction of oxygen molecules and water to form the superoxide radical anion and hydroxyl radical, respectively. Finally, carbon dioxide, water and smaller organic molecules were produced (Umar and Aziz 2013).

Conclusion

The photodegradation rate constants of $8.6 \times 10^{-3} \text{ min}^{-1}$ and $4.3 \times 10^{-3} \text{ min}^{-1}$ were obtained using ZnO NPs grown on microsized sand and unsupported ZnO NPs, respectively. 100% enhancement was obtained using ZnO NPs of similar size. The enhancement was mainly due to the elimination of the possibility of agglomeration of the ZnO NPs which can readily occur in the unsupported sample. The use of sand microparticles provided the advantages of good adhesion of the ZnO NPs and good adsorbance of MB molecules in the vicinity of the ZnO NPs photocatalyst. The supported ZnO NPs afforded a photodegradation efficiency of 71.7% under UV light irradiation for 150 min compared to 48.2% obtained with the unsupported ZnO NPs photocatalyst.

Acknowledgements The authors are grateful to the University of Malaya for the postgraduate research grant (Project Code: PG110-2015A).

Compliance with ethical standards

Conflict of interest The authors declare no conflict of interest regarding the publication of this paper.

Open Access This article is distributed under the terms of the Creative Commons Attribution 4.0 International License (<http://creativecommons.org/licenses/by/4.0/>), which permits unrestricted use, distribution, and reproduction in any medium, provided you give appropriate credit to the original author(s) and the source, provide a link to the Creative Commons license, and indicate if changes were made.

References

- Achak M, Mandi L, Ouazzani N (2009) Removal of organic pollutants and nutrients from olive mill wastewater by a sand filter. *J Environ Manag* 90(8):2771–2779. <https://doi.org/10.1016/j.jenvman.2009.03.012>
- Amna S, Shahrom M, Azman S et al (2015) Review on zinc oxide nanoparticles: antibacterial activity and toxicity mechanism. *Nano-Micro Lett* 7:219–242. <https://doi.org/10.1007/s40820-015-0040-x>
- Bandekar G, Rajurkar NS, Mulla IS et al (2014) Synthesis, characterization and photocatalytic activity of PVP stabilized ZnO and modified ZnO nanostructures. *Appl Nanosci* 4(2):199–208. <https://doi.org/10.1007/s13204-012-0189-2>
- Binks BP, Fletcher PDI, Holt BL et al (2010) Drop sizes and particle coverage in emulsions stabilised solely by silica nanoparticles of irregular shape. *Phys Chem Chem Phys* 12(38):11967–11974. <https://doi.org/10.1039/C0CP00581A>
- Cao G (2004) Nanostructures and nanomaterials: synthesis, properties and applications. World Sci, Singapore
- Dodd AC, McKinley AJ, Saunders M et al (2006) Effect of particle size on the photocatalytic activity of nanoparticulate zinc oxide. *J Nanopart Res* 8(1):43–51. <https://doi.org/10.1007/s11051-005-5131-z>
- Gilbert B, Huang F, Zhang H et al (2004) Nanoparticles: strained and stiff. *Science* 305(5684):651–654. <https://doi.org/10.1126/science.1098454>
- Guo R, Qi J, Luo J et al (2016) A new sintering approach to ceramics at low temperature from Ba (Zr_xTi_{1-x}) O₃ nanoparticles doped by ZnO. *J Adv Ceram* 5(4):277–283. <https://doi.org/10.1007/s40145-017-0219-3>
- Jang ES, Won JH, Hwang SJ, Choy JH (2006) Fine tuning of the face orientation of ZnO crystals to optimize their photocatalytic activity. *Adv Mater* 18(24):3309–3312. <https://doi.org/10.1002/adma.200601455>
- Kuo TJ, Lin CN, Kuo CL, Huang MH (2007) Growth of ultralong ZnO nanowires on silicon substrates by vapor transport and their use as recyclable photocatalysts. *Chem Mater* 19(21):5143–5147. <https://doi.org/10.1021/cm071568a>
- Lin B, Fu Z, Jia Y (2001) Green luminescent center in undoped zinc oxide films deposited on silicon substrates. *Appl Phys Lett* 79(7):943–945. <https://doi.org/10.1063/1.1394173>
- Mamat M, Khusaimi Z, Musa M et al (2010) Novel synthesis of aligned zinc oxide nanorods on a glass substrate by sonicated sol–gel immersion. *Mater Lett* 64(10):1211–1214. <https://doi.org/10.1016/j.matlet.2010.02.053>
- Miao L, Ieda Y, Tanemura S et al (2007) Synthesis, microstructure and photoluminescence of well-aligned ZnO nanorods on Si substrate. *Sci Tech Adv Mater* 8(6):443–447. <https://doi.org/10.1016/j.stam.2007.02.012>
- Mollwo E (1982) Landolt-Börnstein New Series. In: Madelung O, Schulz M, Weiss H (eds) Semiconductors: physics of II–VI and I–VII compounds, semimagnetic semiconductors. Springer, Berlin, p 35
- Nanda K, Maisels A, Kruijs F et al (2003) Higher surface energy of free nanoparticles. *Phys Rev Lett* 91(10):106102. <https://doi.org/10.1103/PhysRevLett.91.106102>
- Noshirvani N, Ghanbarzadeh B, Mokarram RR et al (2017) Preparation and characterization of active emulsified films based on chitosan-carboxymethyl cellulose containing zinc oxide nanoparticles. *Int J Biol Macromolec* 99:530–538. <https://doi.org/10.1016/j.ijbiomac.2017.03.007>
- Ortiz Landeros J, Gómez Yáñez C, López Juárez R et al (2012) Synthesis of advanced ceramics by hydrothermal crystallization and modified related methods. *J Adv Ceram* 1(3):204–220. <https://doi.org/10.1007/s40145-012-0022-0>
- Pung SY, Lee WP, Aziz A (2012) Kinetic study of organic dye degradation using ZnO particles with different morphologies as a photocatalyst. *Int J Inorg Chem* 2012:9. <https://doi.org/10.1155/2012/608183>
- Roduner E (2006) Size matters: why nanomaterials are different. *Chem Soc Rev* 35(7):583–592. <https://doi.org/10.1039/B502142C>
- Sauter C, Emin MA, Schuchmann HP, Tavman S (2008) Influence of hydrostatic pressure and sound amplitude on the ultrasound induced dispersion and de-agglomeration of nanoparticles. *Ultrason Sonochem* 15(4):517–523. <https://doi.org/10.1016/j.ultrasonch.2007.08.010>
- Sun B, Siringhaus H (2006) Surface tension and fluid flow driven self-assembly of ordered ZnO nanorod films for high-performance field effect transistors. *J Am Chem Soc* 128(50):16231–16237. <https://doi.org/10.1021/ja065242z>
- Tang E, Cheng G, Ma X et al (2006) Surface modification of zinc oxide nanoparticle by PMAA and its dispersion in aqueous system. *Appl Surf Sci* 252(14):5227–5232. <https://doi.org/10.1016/j.apsusc.2005.08.004>
- Tao J, Mancl K (2008) Sand size analysis for onsite wastewater treatment system, determination of sand effective size and uniformity coefficient. *Agric Nat Resour*. <https://ohioline.osu.edu/factsheet/aex-757>. Accessed 2 June 2016
- Umar M, Aziz HA (2013) Photocatalytic degradation of organic pollutants in water. In: Rashed MN (ed) Organic pollutants—monitoring, risk and treatment. InTech, Rijeka. <https://doi.org/10.5772/53699>
- Xu J, Chang Y, Zhang Y et al (2008) Effect of silver ions on the structure of ZnO and photocatalytic performance of Ag/ZnO composites. *Appl Surf Sci* 255(5):1996–1999. <https://doi.org/10.1016/j.apsusc.2008.06.130>
- Zhang D, Xue Z, Wang Q (2002) The mechanisms of blue emission from ZnO films deposited on glass substrate by rf magnetron sputtering. *J Phys D Appl Phys* 35(21):2837. <https://doi.org/10.1088/0022-3727/35/21/321>
- Zhang YL, Yang Y, Zhao JH et al (2009) Preparation of ZnO nanoparticles by a surfactant-assisted complex sol–gel method using zinc nitrate. *J Sol-Gel Sci Technol* 51(2):198–203. <https://doi.org/10.1007/s10971-009-1959-5>

Publisher's Note

Springer Nature remains neutral with regard to jurisdictional claims in published maps and institutional affiliations.